Neutron scattering study of magnetic order in single-crystalline $CeCuAl_3$

M. Klicpera,[1,2,*] P. Javorský,[1] P. Čermák,[1,3] A. Schneidewind,[3] B. Ouladdiaf,[2] and M. Diviš[1]

[1]*Charles University in Prague, Faculty of Mathematics and Physics, Department of Condensed Matter Physics, Ke Karlovu 5, 121 16 Prague 2, Czech Republic*

[2]*Institut Laue Langevin, 71 Avenue des Martyrs, CS 20156, 38042 Grenoble Cedex 9, France*

[3]*Jülich Centre for Neutron Science, Forschungszentrum Jülich GmbH, Outstation at Heinz Maier-Leibnitz Zentrum, Lichtenbergstraße 1, 85747 Garching, Germany*

(Received 18 April 2014; revised manuscript received 19 May 2015; published 15 June 2015)

The $CeTX_3$ compounds belong to the intensively studied group of materials revealing such properties as valence fluctuations, heavy-fermion behavior, or pressure-induced superconductivity. So far, magnetic structure was investigated in only a few of these. We performed a series of neutron-diffraction experiments on a structurally well-defined $CeCuAl_3$ single crystal. The ordered non-centro-symmetric tetragonal $BaNiSn_3$-type (*I4mm*) crystal structure as well as the antiferromagnetic order below $T_N \approx 2.7$ K were corroborated by our diffraction experiments. The amplitude modulated magnetic structure with in-plane magnetic moments described by the propagation vector $\mathbf{k} = (0.4, 0.6, 0)$ was revealed. The relation between structural parameters and magnetic structures in the family of isostructural $CeTX_3$ compounds is discussed.

DOI: 10.1103/PhysRevB.91.224419 PACS number(s): 61.05.F−, 71.27.+a, 72.15.Eb, 75.30.Gw

I. INTRODUCTION

Cerium intermetallic compounds have been in the foreground of interest for a few decades. Such physical phenomena as magnetic ordering at very low temperatures, valence fluctuations, heavy-fermion behavior, and unconventional superconductivity have been found and studied in Ce-based compounds so far. The exceptional and often exotic behavior of these Ce-based intermetallics originates in the vicinity of the energy of the cerium $4f$ shell level to the $5d$ and $6s$ levels. The different magnetic properties then arise mainly from the competition between the long-range magnetic order of the Ruderman-Kittel-Kasuya-Yosida (RKKY) type and the screening of the localized cerium $4f$ moments by conduction electrons (the Kondo effect).

The tetragonal $CeTX_3$ or more generally CeT_xX_{4-x} compounds, where T is a transition metal d element and X is a p metal, exhibit various ground states and phenomena depending on the actual chemical composition and/or applied external pressure. Most of these compounds (like $CeRhGe_3$ [1], $CeAuAl_3$ [2], and $CeCoGe_3$ [3]) order antiferromagnetically; several others exhibit ferromagnetic order, e.g., $CeAgAl_3$ [4] and $CeCuGa_3$ [5], or a paramagnetic ground state with valence fluctuations like $CeRuSi_3$ [6]. Spin-glass order is observed in $CePtAl_3$ [7]. The electronic properties of these compounds seem to be rather sensitive to the details of the crystal structure. A possible relation between crystal structure type and magnetic order was discussed in the case of $CeCuGa_3$ [5], where the antiferromagnetic ground state with incommensurate propagation is observed for compounds crystallizing in a $BaNiSn_3$-type structure [8,9], whereas the ferromagnetic order is revealed for $CeCuGa_3$ adopting the $BaAl_4$ type of tetragonal structure [5]. The observation of pressure induced superconductivity in the non-centro-symmetric $BaNiSn_3$-type crystal structure of antiferromagnetically ordered $CeRhSi_3$ and $CeIrSi_3$ [10,11] is particularly remarkable. The recent inelastic neutron-scattering study of $CeCuAl_3$ revealed another highly interesting feature: crystal-field (CF) exciton-phonon interaction leading to a formation of a vibron quasibound state [12].

The magnetic behavior of $CeCuAl_3$ is generally discussed as a result of the interplay between the magnetic RKKY and Kondo interactions [7,12–15]. The magnetic properties are also influenced by the low-lying first excited CF state, splitting between the ground-state and the first excited-state amounts ≈15 K as found by neutron-scattering experiments [12]. The enhanced electronic specific heat at low temperatures characterized by a large γ coefficient is often considered as a sign of the heavy-fermion state in $CeCuAl_3$ [13,14]. However, more detailed analysis which considers this small CF splitting leads to a much smaller γ value, almost comparable with normal metals [16]. $CeCuAl_3$ orders antiferromagnetically with slightly sample dependent Néel temperature $T_N \cong 2.5$–2.9 K [7,13–15]. The nature of the antiferromagnetic ground state was concluded mainly by observing a maximum in the $M(T)$ dependencies [7,13,14]. On the other hand, the magnetization curves do not show any clear signs of behavior that would point to the antiferromagnetic order [17,18]. The final microscopic evidence of the magnetic ground-state nature is still missing, although some preliminary results of neutron diffraction led to the observation of an antiferromagnetic peak described by the $(\frac{1}{2}, \frac{1}{2}, 0)$ propagation vector [19]. To bring an unambiguous proof of the type of the magnetic order and determine the magnetic structure, we have performed a series of neutron-diffraction experiments on a $CeCuAl_3$ single crystal.

II. EXPERIMENT

The single-crystalline $CeCuAl_3$ sample was prepared by the Czochralski pulling method and additionally annealed in quartz tubes at 900 °C for eight days. The details of sample preparation as well as its structural and chemical characterization by differential scanning calorimetry, x-ray, electron and neutron scattering are published in our previous paper [20]. The quality of the $CeCuAl_3$ single crystal was

*mi.klicpera@seznam.cz

proved by our previous Laue neutron-diffraction experiment performed on Orient Express in Institute Laue-Langevin (ILL), Grenoble, France [20]. We stress that all presented measurements were performed on the same single-crystal ingot.

The Laue neutron single-crystal diffraction experiment on $CeCuAl_3$ was performed on the CYCLOPS (Cylindrical CCD Laue Octagonal Photo Scintillator) instrument in ILL. A double octagonal array of neutron CCD detectors covers a cylindrical area of space (see Ref. [21] for more details). The scans were taken at $T = 6$ and 2 K, i.e., in a paramagnetic and magnetically ordered state, respectively. A subsequent neutron-scattering experiment was performed on the PANDA (a cold neutron three axes spectrometer) instrument in Heinz Maier-Leibnitz Zentrum (MLZ), Garching, Germany. The experiment was carried out at temperatures down to 0.45 K using an He^3 insert in closed cycle cryostat. The results of the elastic part of the measurement ($\lambda = 4$ Å) are presented in this paper. The neutron-diffraction experiment on the D10 (a single-crystal four-circle diffractometer with three-axis energy analysis) instrument, ILL, was performed in the final stage of the magnetic structure investigation. A neutron wavelength of $\lambda = 2.36$ Å and two-dimensional microstrip detector were used for the measurement at temperatures down to 1.7 K.

III. RESULTS

At first, the magnetic order in $CeCuAl_3$ was studied by Laue neutron diffraction on the CYCLOPS instrument (ILL). Laue patterns taken at $T = 2$ and 6 K are shown in Fig. 1. The comparison of diffraction patterns obtained in the magnetically ordered state and in the paramagnetic state revealed three weak magnetic reflections at the low Q region indicating a relatively small magnetic moment in the compound. Positions of magnetic satellites out of the Brag reflections unambiguously prove the antiferromagnetic ground state in $CeCuAl_3$. The analysis of the measured Laue patterns (using the Esmeralda software [22]) allows us to determine several possible propagation vectors consistent with our data: (0.2, 0.2, 0), (0.33, 0, 0), (0.5, 0.25, 0), (0.4, 0.4, 0), and (0.4, 0.6, 0). In addition, there are several other incommensurate vectors **k** describing the three observed magnetic reflections as well. However, none of the determined vectors coincides with the propagation of $(\frac{1}{2}, \frac{1}{2}, 0)$ reported in the work of Oohara *et al.* [19].

A further step in the search for the correct propagation vector was carried out in the course of our neutron-scattering experiment on the PANDA spectrometer (MLZ). The mapping of the reciprocal space revealed several magnetic reflections (two of them shown in Fig. 2), which are described unambiguously by the propagation vector $\mathbf{k} = (0.4, 0.6, 0)$. All other possible propagation vectors determined from CYCLOPS data were excluded. The temperature dependence of the intensity on the magnetic reflection $(0.6, -0.4, 0)$ is shown in Fig. 3. The ordered magnetic moment on Ce sites increases with decreasing temperature down to $\approx$1.7 K and remains constant (within the measurement error) at lower temperatures. The fit of the magnetic intensity to the power law $I \sim (T_N - T)^{2\beta}$ revealed the ordering temperature of $T_N = 2.7$ K, corresponding well to T_N obtained from

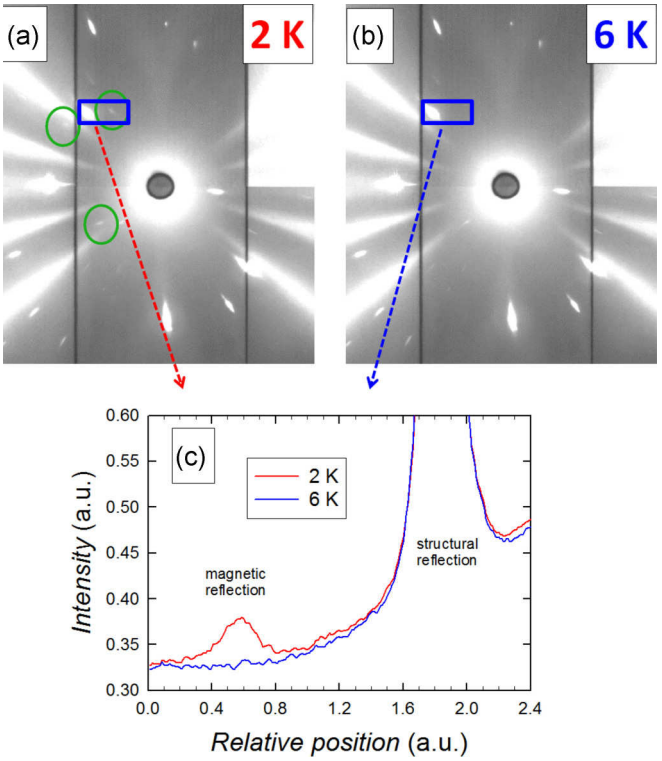

FIG. 1. (Color online) The Laue patterns obtained at 2 and 6 K by the CYCLOPS instrument in ILL, Grenoble. Three magnetic reflections are marked by green circles in panel (a). The integrated intensities calculated by the Esmeralda program [22] from Laue patterns are shown in panel (c).

macroscopic measurements [7,13–15]. The fitted value of the critical exponent $\beta = 0.4$ is relatively close to the theoretical value of 0.313 expected for the Ising three-dimensional system [23].

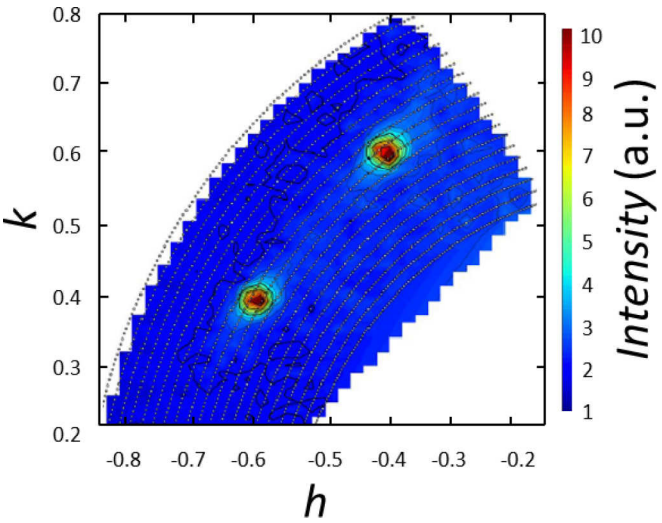

FIG. 2. (Color online) The map of the hk plane obtained by measurement on the PANDA instrument in MLZ, Garching. Clear magnetic reflections $(-0.6, 0.4, 0)$ and $(-0.4, 0.6, 0)$ are observed.

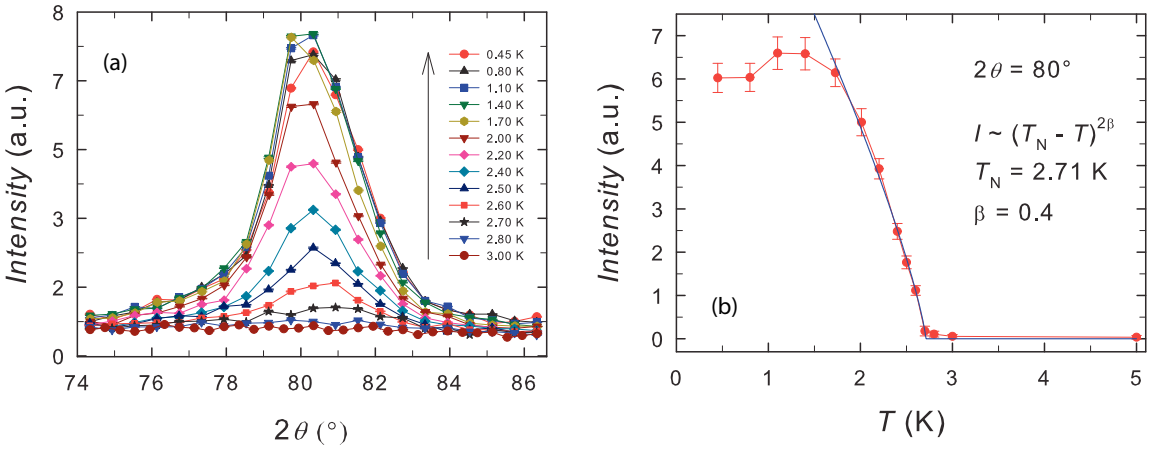

FIG. 3. (Color online) Temperature dependence of intensity on magnetic reflection (0.6, −0.4, 0). The error bars in panel (a) are within the symbols. The blue curve in panel (b) is a fit of the data to $I \sim (T_N - T)^{2\beta}$. See text for more details.

The determined propagation vector $\mathbf{k} = (0.4, 0.6, 0)$ (and structure parameters from Ref. [20]) was used to calculate possible magnetic structures by representation analysis employing the program BasIreps [24]. It should be noted that there is only one crystallographic site for the Ce atom per magnetic unit cell. The calculation revealed two irreducible representations. Three basis vectors (1, −1, 0), (1, 1, 0), and (0, 0, 1) belong to these representations where the latter two belong to the same irreducible representation. The representation containing only one basis vector corresponds to moments arranged within the basal plane. The second irreducible representation with more than one basis vector contains also any linear combination of these vectors. The second representation thus allows any direction of magnetic moments with respect to the c axis.

For the final magnetic structure determination based on a propagation vector $\mathbf{k} = (0.4, 0.6, 0)$ a neutron-diffraction experiment on the D10 diffractometer (ILL) was performed. We should note that the $BaNiSn_3$-type structure (*I4mm*, 107) is a non-centro-symmetric structure, therefore the propagation vectors $\mathbf{k}$ and $-\mathbf{k}$ are not equivalent. Both vectors as well as propagation vectors (0.4, −0.6, 0) and (−0.4, 0.6, 0) had to be taken into account during the data refinement. The magnetic structure refinement was preceded by thorough inspection of the crystal structure, based on measurement of 24 nuclear reflections. All observed reflections satisfied the condition $h + k + l = 2n$, confirming the body-centered space group. The intensities of nuclear reflections measured in the paramagnetic and in the ordered state (at 1.7 K) remain unchanged, excluding clearly the $\mathbf{k} = (0, 0, 0)$ propagation vector in $CeCuAl_3$. The measured data were analyzed using the Fullprof program [24]. The extinction in the sample was treated by fitting the nuclear data to the phenomenological Zachariasen formula [25], using six fitting parameters describing anisotropy in the crystal lattice [24]. The consideration of extinction during the Rietveld refinement leads to the significant decrease of the R_F factor from 5.3 to 1.7%. The obtained parameters were fixed for the fit of magnetic data. Any absorption of the material was not taken into account during the fitting as the intensity on equivalent reflections was the same within experimental error; $CeCuAl_3$ does not contain any strongly absorbing element.

The intensities of magnetic satellites described by the propagation vector $\mathbf{k} = (0.4, 0.6, 0)$ were subsequently measured at 1.7 K. The integrated intensities $|F_{meas}|$ of 25 independent magnetic reflections are listed in Table I. All these magnetic reflections are the satellites of allowed nuclear reflections (described by $h + k + l = 2n$); zero intensity was found on satellites of forbidden nuclear reflections ($h + k + l = 2n + 1$). The measured data were fitted to the

TABLE I. 25 magnetic reflections with measured integrated intensities $|F_{meas}|$. $|F_{calc}|$ represents the calculated intensity processed by the Fullprof program [24] for the magnetic structure presented in Fig. 4.

h	k	l	$\lvert F_{meas}\rvert$	$\lvert F_{calc}\rvert$
0.4	0.4	1	23(1)	21.3
−0.4	−0.4	1	25(1)	21.3
0.4	1.4	0	15(4)	12.6
−0.4	0.6	0	61(7)	61.2
0.6	0.6	1	13(1)	11.1
−0.6	−0.6	1	18(1)	11.1
0.4	−0.6	2	55(3)	58.3
−0.4	−1.4	2	22(3)	20.6
0.4	0.4	3	46(1)	45.5
−0.4	−0.4	3	50(1)	45.4
−0.6	1.4	3	39(2)	41.2
−1.4	0.6	3	40(3)	41.2
1.4	0.4	2	22(2)	20.6
0.6	−0.4	2	55(4)	58.3
1.4	−0.6	1	40(3)	44.8
0.6	−1.4	1	39(1)	44.8
0.6	0.6	3	31(1)	35.5
−0.6	−0.6	3	36(1)	35.5
1.6	−0.4	1	36(4)	37.0
−1.6	0.4	1	33(5)	37.0
−0.4	0.6	4	53(7)	48.0
0.4	−0.6	4	54(3)	48.0
−0.4	1.6	3	39(2)	35.7
0.4	−1.6	3	39(3)	35.7
0.6	1.6	0	16(5)	8.4

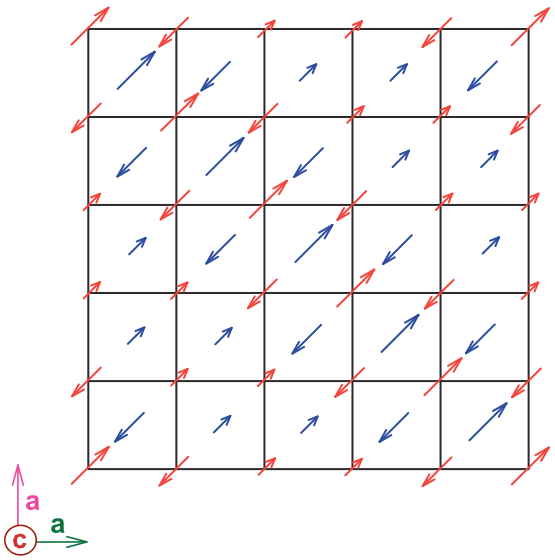

FIG. 4. (Color online) The magnetic structure of $CeCuAl_3$ described by propagation vector $\mathbf{k} = (0.4, 0.6, 0)$. Red arrows symbolize magnetic moments at $z = 0$; blue arrows symbolize moments at $z = \frac{1}{2}$. All moments lie within the basal plane. See text for further details.

model of magnetic structures based on the results of representation analysis described above. While the existence of magnetic domains was considered, multi-**k** magnetic structures are very unlikely in the case of $CeCuAl_3$.

The by far best agreement between the data and the fit ($R_F = 5.2\%$, see calculated intensities $|F_{calc}|$ in Table I) was obtained for magnetic structure with an arrangement of magnetic moments described by the basis vector (1, 1, 0). The model using the (1, − 1,0) basis vector gives an unacceptable fit with $R_F = 35.6\%$. The determined magnetic structure is of an amplitude modulated type with moments lying within the basal plane and reaching a maximum value of 0.28(1) μ_B/Ce^{3+}; see Fig. 4. As follows from the representation analysis, any linear combination of (1, 1, 0) and (0, 0, 1) basis vectors should be considered. For the nonzero component described by (0, 0, 1) this would lead to a tilt of the moments out of the basal plane. Allowing a free z component does not lead to any significant improvement of the fit and converges to a zero value of the z component in the refinement. We should note that allowing a subtle leaning of magnetic moments within the basal plane away from the [110] crystallographic direction leads to a somewhat better agreement factor of $R_F = 4.3\%$. The determined amplitude modulated magnetic structure with strongly reduced magnetic moments lying within the basal plane is well consistent also with results of previous ^{27}Al nuclear quadrupole resonance (NQR) study [26].

IV. DISCUSSION

Let us comment first on the discrepancy between our results and the previous study of Oohara *et al.* [19]. The propagation vector $(\frac{1}{2}, \frac{1}{2}, 0)$ found by their former neutron-diffraction experiment is clearly not reproduced in any of our three independent neutron experiments; the agreement is only that the propagation vector lies within the *ab* plane ($k_z = 0$). Some differences in the crystal structure and/or sample quality may be a reason for the different propagation vector. The $CeCuAl_3$ crystal used by Oohara *et al.* was originally reported to crystallize in the $BaAl_4$-type superlattice [14] without further details concerning, e.g., atomic positions and occupancies. The experiments in our present work were performed on a structurally well-described single crystal with the tetragonal ordered non-centro-symmetric $BaNiSn_3$-type structure [20]. Moreover, during our experiments on PANDA and D10 instruments, we investigated the possibility of another magnetic propagation vector as presented in Ref. [19]. Tiny peaks corresponding to the reflections (0.5, 0.5, 0) and (−0.5, 0.5, 0) were found. The intensities of these peaks were considerably weaker than the ones described by propagation vector (0.4, 0.6, 0) as shown in Fig. 2 [the peak described as (−0.5, 0.5, 0) is below the visible scale]. Nevertheless, we have examined these $(\frac{1}{2}, \frac{1}{2}, 0)$ peaks at temperatures $1.7 \leqslant t \leqslant 200$ K and no change of the intensity was observed in the whole temperature interval, while the peaks described by $\mathbf{k} = (0.4, 0.6, 0)$ disappeared at a temperature of 2.7 K (as demonstrated in Fig. 3). $\frac{\lambda}{2}$ contamination from the (1, 1, 0) nuclear reflection might be a certain source of intensity on these obviously nuclear peaks. However, Oohara *et al.* [19] presented the temperature development of the observed peak, which is in a strong disagreement with $\frac{\lambda}{2}$ contamination; this temperature evolution was not reproduced by our study. The structural difference thus remains the only explanation.

The measurements employing the inelastic neutron scattering on $CeCuAl_3$ [12] and $CeAuAl_3$ [27] strongly corroborate our results. The crystal-field parameters obtained for both isoelectronic and isostructural compounds—$B_2^0 = 0.611$ meV, $B_4^0 = -0.015$ meV, and $|B_4^4| = 0.317$ meV for $CeCuAl_3$ and $B_2^0 = 1.2036$ meV, $B_4^0 = -0.0031$ meV, and $|B_4^4| = 0.4269$ meV for $CeAuAl_3$—lead to the same type of magnetic anisotropy with magnetic moments arranged within the basal plane for both compounds. Indeed, our present study on $CeCuAl_3$ as well as previous investigation of $CeAuAl_3$ [27] reveal the magnetic moments to be confined within the basal plane. The magnetic structures are thus fully consistent with reported CF parameters. The $CeCuAl_3$ study of Oohara *et al.* [19] yields to magnetic moments aligned along the c axis, which is in strong disagreement with the CF anisotropy [12] and also with our study.

The value of the magnetic moment in $CeCuAl_3$ [0.28(1) μ_B/Ce^{3+}] is significantly reduced compared to the full Ce^{3+} moment. Such a small ground-state magnetic moment is not exceptional among $CeTX_3$ compounds adopting the $BaNiSn_3$-type structure. $CeCoGe_3$ reveals the magnetic moment of 0.405 μ_B/Ce^{3+} [3], and $CeRhGe_3$ reveals the moment of 0.45 μ_B/Ce^{3+} [1]. An even smaller value of the magnetic moment (0.13 μ_B/Ce^{3+}) was found in $CeRhSi_3$ [28] and a similar value is predicted also for $CeIrSi_3$ [29]. On the other hand, $CeCuGa_3$ (1.24 μ_B/Ce^{3+}) [9] and $CeAuAl_3$ (1.05 μ_B/Ce^{3+}) [27] reveal significantly higher magnetic moments. The small value of the magnetic moment in these $CeTX_3$ compounds is often associated to the influence of the Kondo effect on long-range magnetic ordering. However, the Néel temperature and Kondo temperature are similar for all $CeTX_3$ compounds, which would propose a similar reduction of the magnetic moment due to the Kondo screening. Thus,

the Kondo screening is unlikely to be the single origin of the significantly different values of magnetic moments within the CeTX_3 family and other mechanisms have to be taken into account. The influence of crystal field plays an important role; however, the reduction of the magnetic moment due to CF effects is unlikely to be so strong (the values of magnetic moments based on CF calculations are slightly higher than 1 μ_B/Ce^{3+} for the above listed compounds). The previous ^{27}Al NQR studies on $CeCuAl_3$ [26] and nuclear magnetic resonance studies on $CeAuAl_3$ [30] brought a significant piece of information about the reason of such different sizes of magnetic moments in these compounds. While the Ce magnetic moment is predicted to be reduced by about 25% due to Kondo screening in $CeAuAl_3$ [30], $CeCuAl_3$ should exhibit a much smaller magnetic moment (<0.2 μ_B/Ce^{3+}) due to a cancellation of the respective internal fields from nearest-neighbor Ce moments [26]. Indeed, the neutron-scattering study on $CeAuAl_3$ [27] revealed a significantly higher magnetic moment than that in $CeCuAl_3$, in agreement with resonance predictions. This agreement shows that the interatomic distances play a crucial role in the formation of the magnetic ground state. The reason behind these significantly different sizes of magnetic moments in CeTX_3 compounds needs to be further investigated, though. Presumably, the combination of neutron-scattering and nuclear magnetic resonance techniques would bring proper explanation.

When comparing the magnetic propagation vectors within the CeTX_3 family of non-centro-symmetric $BaNiSn_3$-type structure compounds, one can distinguish three different types of propagation. $CeCuAl_3$ [$\mathbf{k} = (0.4, 0.6, 0)$] and $CeCuGa_3$ [$\mathbf{k} = (0.176, 0.176, 0)$] [9] form the first group, in which the magnetic moments lie within the basal plane and the antiferromagnetic propagation occurs also within the basal plane. The second group is formed by compounds with magnetic structure characterized by propagation vectors ($k_x = k_y = 0$, $k_z \neq 0$), i.e., the magnetic moments form ferromagnetic planes which propagate antiferromagnetically along the c axis. $CeCoGe_3$ with $\mathbf{k} = (0, 0, \frac{1}{2})$ [3], $CeRhGe_3$ with $\mathbf{k} = (0, 0, \frac{3}{4})$ [1], and recently investigated $CeAuAl_3$ with $\mathbf{k} = (0, 0, 0.52)$ [27] belong to this group. The last part of the CeTX_3 family crystallizing in the $BaNiSn_3$-type structure contains compounds with more complex magnetic structures described by more general propagation vectors: $CeRhSi_3$ and $CeIrSi_3$ show the propagation vectors (0.218, 0, 0.5) and (0.265, 0, 0.43), respectively [28,29]. The systematics in the propagation of magnetic moments in these compounds is not obvious so far. One might expect that the lattice parameters would play an important role in the magnetic structure formation. The c/a ratio itself does not seem to be the only driving parameter—rather close values of $c/a = 2.48$ and 2.51 are found for $CeAuAl_3$ and $CeCuAl_3$ compounds showing different propagation direction [20,27]. The c/a ratio in CeTGe_3 and CeTSi_3 takes the value of $\approx$2.3 [1,3,28,29] and these compounds exhibit a propagation vector with z component $k_z \neq 0$.

The nearest interatomic Ce-Ce distance (i.e., lattice parameter a) seems to be crucial for the ordering of magnetic moments in CeTX_3 compounds: $CeCuAl_3$ [20] and $CeCuGa_3$ [9] with $k_z = 0$ exhibit nearest Ce-Ce neighbors distances lower than 4.3 Å, whereas $CeCoGe_3$, [3] $CeRhGe_3$ [1], and

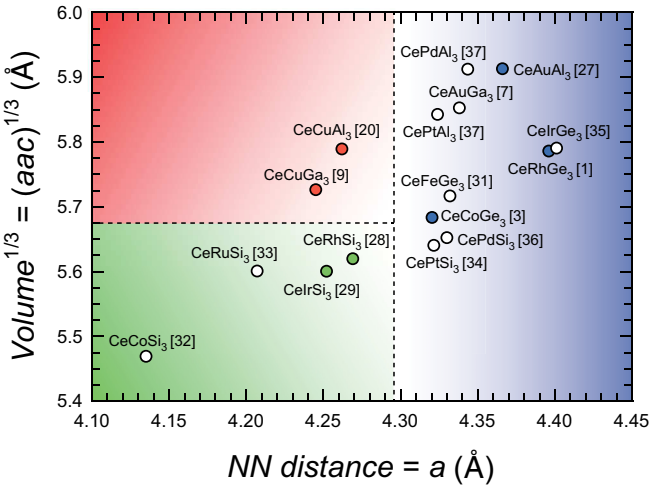

FIG. 5. (Color online) The lattice parameters of CeTX_3 compounds. Nearest Ce-Ce neighbors distance, i.e., lattice parameter a vs the cube root of volume of elemental unit cell $(aac)^{\frac{1}{3}}$, is shown. The colored symbols mark the type of magnetic propagation vector as discussed in text: The red symbol belongs to the compounds with a zero z component of the magnetic propagation vector, the blue symbol belongs to the compounds with ($k_x = k_y = 0$, $k_z \neq 0$), and the green symbol marks the compounds with more complex propagation vectors. White circles denote compounds with not yet revealed magnetic structures. The colored areas accordingly denote predicted propagation in other CeTX_3 compounds [31–37].

$CeAuAl_3$ [27] with $a > 4.3$ Å propagate along the tetragonal axis ($k_z \neq 0$). In the third group formed by $CeRhSi_3$ [28] and $CeIrSi_3$ [29], both a and c are relatively small (i.e., small lattice volume), which brings the second-nearest Ce-Ce neighbors significantly closer to each other ($\approx$ 5.7 Å, compared to $\approx$6.1 Å for $CeCuAl_3$ [20] and $CeCuGa_3$ [9]) and probably has some impact on the magnetic propagation. We are aware that the tentative considerations above are based on the knowledge of magnetic structures only in a rather limited number of compounds. We have constructed a phase diagram of CeTX_3 compounds based on the above considerations (Fig. 5) dividing CeTX_3 compounds into three groups according to their lattice parameter a (i.e., nearest interatomic Ce-Ce distance) and volume of elementary unit cell. This arrangement respects the type of magnetic propagation vector in all previously studied compounds. The predictions of the type of magnetic propagation vector for other CeTX_3 compounds have to be confirmed by future neutron-diffraction experiments.

V. CONCLUSIONS

A series of neutron-diffraction experiments was performed on a structurally well-defined $CeCuAl_3$ single crystal. $CeCuAl_3$ reveals an antiferromagnetic ground state below $T_N = 2.7$ K without any further phase transition down to 0.4 K. The amplitude modulated magnetic structure is described by propagation vector $\mathbf{k} = (0.4, 0.6, 0)$. The magnetic moments are arranged within the basal plane along the [110] crystallographic direction with a maximum value of 0.28 μ_B/Ce^{3+}. The magnetic structure of $CeCuAl_3$ was put

into the context of other $CeTX_3$ compounds and the overall mechanism of the magnetic structure formation was proposed.

ACKNOWLEDGMENTS

The preparation and characterization of the $CeCuAl_3$ single crystal were performed in MLTL (http://mltl.eu/), which is supported within the program of Czech Research Infrastructures (Project No. LM2011025). The work of M.K. was supported by a grant agency of Charles University under Project No. 76213. We acknowledge Institute Laue-Langevin, Grenoble, France, for the allocation of time on CYCLOPS and D10 instruments and technical services. This work is a part of Research Project No. LG14037 financed by the Ministry of Education, Youth, and Sports, Czech Republic. This work is based upon experiments performed on the PANDA instrument operated by the Jülich Centre for Neutron Science at Heinz Maier-Leibnitz Zentrum, Garching, Germany. This research project has been supported by the European Commission under the Seventh Framework Program through the Research Infrastructures action of the Capacities Program No. NMI3-II Grant No. 283883.

[1] A. D. Hillier, D. T. Adroja, P. Manuel, V. K. Anand, J. W. Taylor, K. A. McEwen, B. D. Rainford, and M. M. Koza, Phys. Rev. B **85**, 134405 (2012).
[2] S. Paschen, E. Felder, and H. R. Ott, Eur. Phys. J. B **2**, 169 (1998).
[3] M. Smidman, D. T. Adroja, A. D. Hillier, L. C. Chapon, J. W. Taylor, V. K. Anand, R. P. Singh, M. R. Lees, E. A. Goremychkin, M. M. Koza, V. V. Krishnamurthy, D. M. Paul, and G. Balakrishnan, Phys. Rev. B **88**, 134416 (2013).
[4] T. Muranaka and J. Akimitsu, Physica C **460–462**, 688 (2007).
[5] Devang A. Joshi, P. Burger, P. Adelmann, D. Ernst, T. Wolf, K. Sparta, G. Roth, K. Grube, C. Meingast, and H. v. Löhneysen, Phys. Rev. B **86**, 035144 (2012).
[6] P. Haen, P. Lejay, B. Chevalier, B. Lloret, J. Etourneau, and M. Sera, J. Less Common Met. **110**, 321 (1985).
[7] S. Mock, C. Pfleiderer, H. v. Lohneysen, J. Low Temp. Phys. **115**, 1 (1999).
[8] J. M. Martin, D. M. Paul, M. R. Lees, D. Werner, and E. Bauer, J. Magn. Magn. Mater. **159**, 223 (1996).
[9] J. M. Martin, M. R. Lees, D. McK. Paul, P. Dai, C. Ritter, and Y. J. Bi, Phys. Rev. B **57**, 7419 (1998).
[10] N. Kimura, K. Ito, K. Saitoh, Y. Umeda, H. Aoki, and T. Terashima, Phys. Rev. Lett. **95**, 247004 (2005).
[11] I. Sugitani, Y. Okuda, H. Shishido, T. Yamada, A. Thamhavel, E. Yamamoto, T. D. Matsuda, Y. Haga, T. Takeuchi, R. Settai, and Y. Ōnuki, J. Phys. Soc. Japan **75**, 043703 (2006).
[12] D. T. Adroja, A. del Moral, C. de la Fuente, A. Fraile, E. A. Goremychkin, J. W. Taylor, A. D. Hillier, and F. Fernandez-Alonso, Phys. Rev. Lett. **108**, 216402 (2012).
[13] E. Bauer, N. Pillmayr, E. Gratz, G. Hilscher, D. Gignoux, and D. Schmitt, Z. Phys. B **67**, 205 (1987).
[14] M. Kontani, H. Ido, H. Ando, T. Nishioka, and Y. Yamaguchi, J. Phys. Soc. Japan **63**, 1652 (1994).
[15] T. Nishioka, Y. Kawamura, H. Kato, M. Matsumura, K. Kodama, and N. K. Sato, J. Magn. Magn. Materials **310**, e12 (2007).
[16] S. A. M. Mentink, N. M. Bos, F. J. van Rossum, G. J. Nieuwenhuys, J. A. Mydosh, and K. H. J. Buschow, J. Appl. Phys. **73**, 6625 (1993).
[17] M. Kontani, G. Motoyama, T. Nishioka, and K. Murase, Physica B **259–261**, 24 (1999).
[18] M. Klicpera, P. Javorský, and M. Diviš, J. Phys.: Confer. Series **592**, 012014 (2015).
[19] Y. Oohara, G. Motoyama, T. Nishioka, and M. Kontani, ISSP Series A Technical Report No. 3526, 1999 (unpublished).
[20] M. Klicpera, P. Javorský, P. Čermák, A. Rudajevová, S. Daniš, T. Brunátová, and I. Císařová, Intermetallics **46**, 126 (2014).
[21] B. Ouladdiaf, J. Archer, J. R. Allibon, P. Decarpentrie, M. H. Lemée-Cailleau, J. Rodriguez-Carvajal, A. W. Hewat, S. York, D. Brau, and G. J. McIntyre, J. Appl. Crystall. **44**, 392 (2011).
[22] J. Rodriguez-Carvajal, L. Fuentes-Montero, and P. Čermák (unpublished), http://lauesuite.com/.
[23] G. S. Brush, Rev. Mod. Phys. **39**, 883 (1967).
[24] J. Rodriguez-Carvajal, Physica B **192**, 55 (1993).
[25] W. H. Zachariasen, Acta Crystallogr. **23**, 558 (1967).
[26] M. Matsumura, Y. Kawamura, M. Yoshina, T. Nishioka, and H. Kato, J. Phys.: Confer. Series **150**, 042122 (2009).
[27] D. T. Adroja, C. de la Fuente, A. Fraile, A. D. Hillier, A. Daoud-Aladine, W. Kockelmann, J. W. Taylor, A. P. Murani, M. M. Koza, E. Burzurí, F. Luis, J. I. Arnaudas, and A. del Moral, arXiv:1501.00286.
[28] N. Aso, H. Miyano, H. Yoshizawa, N. Kimura, T. Komatsubara, and H. Aoki, J. Magn. Magn. Mater. **310**, 602 (2007).
[29] N. Aso, M. Takahashi, H. Yoshizawa, H. Iida, N. Kimura, and H. Aoki, J. Phys.: Conf. Series **400**, 022003 (2012).
[30] P. Vonlanthen, J. L. Gavilano, B. Ambrosini, and H. R. Ott, Eur. Phys. J. B **7**, 9 (1999).
[31] H. Yamamoto, H. Sawa, and M. Ishikawa, Phys. Lett. A **196**, 83 (1994).
[32] J. B. Hong, J. W. Kim, K. E. Lee, N. A. Lee, K. H. Jang, J.-G. Park, and Y. S. Kwon, J. Magn. Magn. Mater. **310**, 292 (2007).
[33] Yu. D. Seropegin, B. I. Shapiev, A. V. Gribanov, and O. I. Bodak, J. Alloys Comp. **288**, 147 (1999).
[34] T. Kawai, Y. Okuda, H. Shishido, A. Thamizhavel, T. D. Matsuda, Y. Haga, M. Nakashima, T. Takeuchi, M. Hedo, Y. Uwatoko, R. Settai, and Y. Onuki, J. Phys. Soc. Japan **76**, 014710 (2007).
[35] T. Kawai, H. Muranaka, M.-A. Measson, T. Shimoda, Y. Doi, T. D. Matsuda, Y. Haga, G. Knebel, G. Lapertot, D. Aoki, J. Flouquet, T. Takeuchi, R. Settai, and Y. Onuki, J. Phys. Soc. Japan **77**, 064716 (2008).
[36] Yu. D. Seropegin, A. V. Gribanov, O. L. Kubarev, A. I. Tursina, and O. I. Bodak, J. Alloys Comp. **317–318**, 320 (2001).
[37] Ch. Franz, Ph.D. thesis, Technical University of Munich, 2014.